Proceedings of the 11th World Congress on Electrical Engineering and Computer Systems and Sciences (EECSS'25)
Paris, France - August, 2025
Paper No. EEE 136
DOI: 10.11159/eee25.136

Comparative Analysis of Nature-Inspired Optimization Algorithms for Partial Shading Conditions

Imran Semanur Arpacı[1], Enes Ladin Öncül[2], Ozgun Girgin[3]
[1]Department of Physics Engineering, Istanbul Technical University
ITU Ayazaga Campus, 34469, Istanbul/Turkiye
arpaci20@itu.edu.tr; oncul17@itu.edu.tr; ogirgin@itu.edu.tr

Abstract **-** Photovoltaic (PV) systems have gained significant attention as a sustainable energy source, but their efficiency is highly dependent on environmental conditions. Under Partial Shading Conditions (PSC), multiple power peaks occur, making conventional Maximum Power Point Tracking (MPPT) techniques ineffective. To address this, several nature-inspired optimization algorithms have been developed, including Particle Swarm Optimization (PSO), Adaptive PSO, Cuckoo Search (CS), Flower Pollination Algorithm (FPA), Grey Wolf Optimizer (GWO), Horse Herd Optimization (HHO), and Hybrid PO-PSO. This study presents a comparative analysis of these algorithms in terms of tracking efficiency and robustness under dynamic shading patterns. PSO and its adaptive variant show fast convergence but may suffer from local optima. CS and FPA offer improved exploration capabilities, whereas GWO and HHO demonstrate better stability in complex landscapes. The Hybrid PO-PSO approach integrates the benefits of PO and PSO, achieving enhanced performance. Simulation results validate the effectiveness of each algorithm in extracting the maximum available power under different PSC scenarios. The analysis provides insights into the optimal selection of MPPT techniques for improving the reliability and efficiency of PV systems.

Keywords**:** MPPT , Partial Shading, Optimization Algorithms, Particle Swarm Optimization, Cuckoo Search, Flower Pollination, Grey Wolf Optimizer, Hybrid PO-PSO

1. Introduction

In [1], the study addresses PV efficiency under partial shading, highlighting multi-peak P–V curves. It notes boost converter efficiency varies with input voltage, shifting the load's MPP from the array's. Simulations and experiments validate power transfer analysis across shading patterns. The focus is on maximizing load power rather than array MPP. In [2], a review targets PV parameter estimation and MPPT to boost energy conversion ratio (ECR). Analytical methods falter due to singularity, and iterative ones struggle with dynamic conditions. Evolutionary algorithms (GA, PSO, DE) excel by avoiding local minima. It advocates these for precise, swift parameter estimation under varying irradiation. In [3], a two-diode PV model with four factors is proposed for PSC accuracy. It outperforms Neural Network, PO, and single-diode models, especially at low irradiance. Real-time simulator data validates its precision for large-array simulations. The model integrates seamlessly with MPPT and converters. In [4], MPPT algorithms are classified into four groups: optimization, hybrid, modelling, and topologies. It reviews PV modelling, array setups, and controllers for PSC system design. Each approach's trade-offs are outlined concisely. The work serves as a practical reference for PV professionals. In [5], 62 MPPT algorithms are detailed across seven categories, including 25 meta-heuristic types. These are subdivided into biology-, physics-, and sociology-based methods. It provides a granular, application-specific guide for PSC optimization. The review is a comprehensive resource for tailored PV solutions.

In [6], the study examines PV module behaviour under PSC, noting multiple local MPPs and one global MPP. It compares PSO and CS against the conventional INR-based tracker using MATLAB simulations. Results show PSO and CS ensure global MPP convergence, with CS outperforming PSO by reducing tracking time across all shading patterns. This highlights CS's superiority in optimization efficiency for PSC. In [7], a hybrid MPPT for large PV schemes at PSC integrates PSO for initial tracking with PO for final stages. Simulated across two PV configurations and validated experimentally via microcontroller, it achieves faster global MPP convergence than standalone PSO or PO. The method also minimizes oscillations in power, voltage, and current, enhancing stability. In [8], a review focuses on improving conventional MPPT methods (PO, hill climbing, incremental conductance) for global MPP tracking under PSC. This

provides a comparative framework for selecting optimal MPPT techniques. In [9], the study addresses PSO's limitations in tracking global MPP under dynamic PSC, where shading changes affect peak location and value. It proposes reinitializing particles for sudden changes and a novel adaptive strategy for gradual shifts, unaddressed in prior literature. Results validate the strategy's ability to consistently catch the global peak. This introduces a pioneering approach to adaptive metaheuristic tracking. In [10], the work explores PSC impacts on building-integrated PV systems (BIPVPS), deeming traditional MPPT inadequate. It introduces the FPA for global MPP tracking, validated across shading arrangements and assessed with differential evolution and PSO. FPA excels in precision and performance, offering a robust solution for BIPVPS optimization.

In [11], a new MPPT procedure employing FPA method enhanced with Levy flight is proposed to tackle multi-peak P–V curves under partial shading. Implemented in MATLAB, it outperforms two established MPPT methods in tracking speed and effectiveness. The method quickly adapts to environmental changes, ensuring global MPP convergence. This underscores FP's potential with advanced convergence mechanisms. In [12], the HHO, inspired by horse herd behaviour, is introduced to maximize PV output under partial and complex shading. Compared to P44O, Adaptive ACS, PSO, and Dragonfly Algorithm (DA), HOA excels in computational efficiency, fast convergence, and zero oscillations. It outperforms conventional methods across varied weather conditions. This highlights HOA's robustness for dynamic shading scenarios. In [13], the failure of the PO procedure under PSC, where multiple peaks emerge, is analyzed. A new HHO procedure is presented to trace the global peak, validated via MATLAB simulations of PV's characteristics. HH's efficacy is compared with other optimization methods, proving superior global peak tracking. This emphasizes HH's role in overcoming PO's limitations. In [14], a hybrid MPPT merging PSO and PO is proposed for PV schemes under uniform and PSC, modelled in PSIM software. Compared to classical PO, standard PSO, and PO-PSO hybrid, it achieves better tracking than standard PSO and extracts 0.3% more power than PO-PSO. The method ensures global MPP under diverse conditions. This demonstrates the value of hybrid optimization for efficiency gains. In [15], a hybrid MPPT merges stochastic PSO with deterministic hill climbing for PV systems under partial shading. PSO optimizes dynamically, with hill climbing refining the best particle's position and a re-randomization mechanism placing five particles strategically. This enhances global MPP tracking in shaded conditions. The approach balances exploration and precision effectively.

PSC in PV systems introduce multi-peak P–V curves, complicating MPPT . Various MPPT procedures extending from traditional methods like PO to developed evolutionary procedures such as PSO, CS, FPA, and HHO, as well as hybrid approaches—each exhibit distinct merits and demerits. While conventional methods struggle with local optima and slow convergence, metaheuristic algorithms excel in global MPP tracking but may face issues like computational complexity or tracking delays under dynamic shading. Hybrid methods aim to balance speed and accuracy but vary in stability and efficiency. This paper compares the working of these diverse MPPT techniques under PSC, analyzing their effectiveness in terms of tracking speed, accuracy, convergence to the global MPP (GMPP), and stability. By evaluating their strengths and limitations, the study aims to determine which MPPT method performs best under PSC, providing a clear guide for optimizing PV system efficiency in real-world shading scenarios

2. System Description

A PV module with a Boost regulator and MPPT Control is represented in the Fig.1. To produce DC voltage and current, the PV module is made up of many PV panels linked in series and parallel. The MPPT algorithm block receives the PV array parameters, which include V_{pv}, I_{pv}, irradiance (G), and temperature (T). It uses a number of optimization strategies, including PSO, Adaptive PSO, CSA, FPA, GWO, HHO, and Hybrid PO-PSO. The MPPT procedure's goal is to maximize power extraction across a range of weather changes by dynamically vary the boost regulators duty cycle to assure the PV system runs at its maximum power point (MPP).

The PV modules voltage is increased by the boost regulator, a power conversion circuit, before it is sent to the load. For energy storage and voltage control, it is made up of an inductor, a switch (S), diode and a capacitor (C). The MPPT method provides the PWM generator with the ideal duty cycle, which it uses to manage power conversion effectively by controlling transistor (S) switching. The load receives the boost converter's processed DC output, guaranteeing steady

and improved energy supply for a range of uses, including freestanding loads, grid-connected systems, and battery storage.

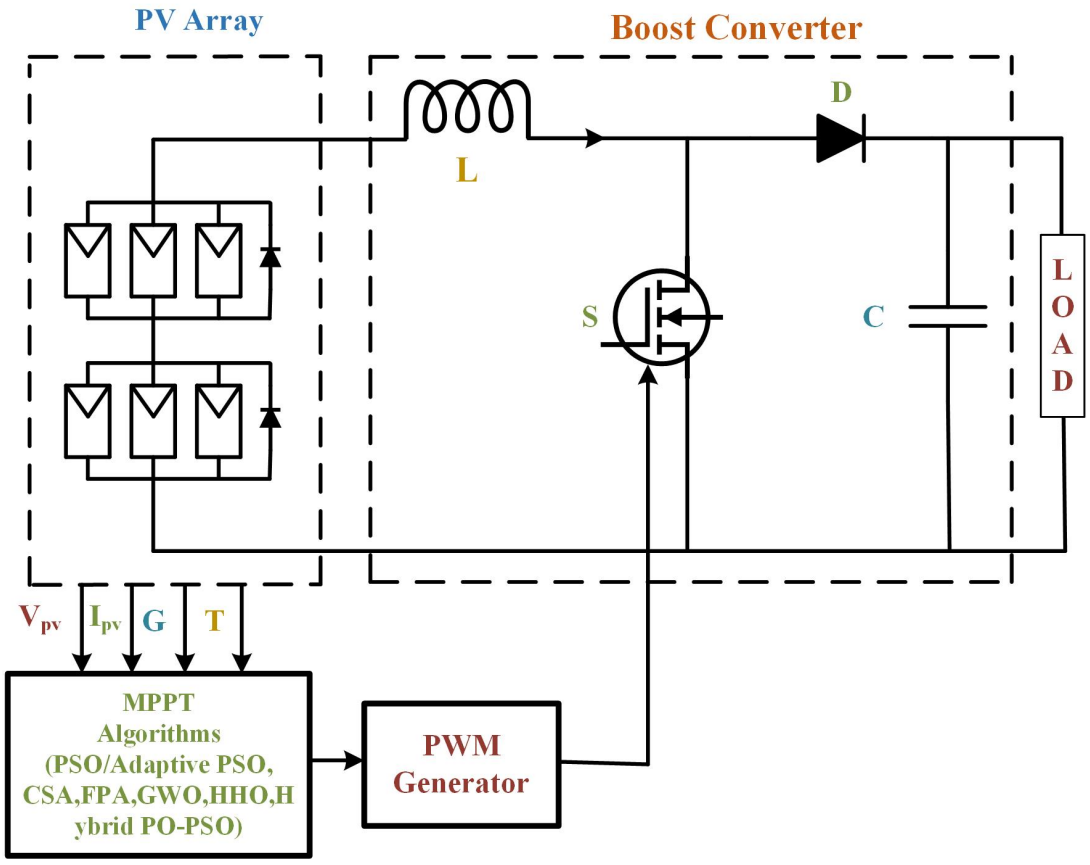

Fig.1 Overall representation of the system

2.1 PV Modelling

The most often used mathematical description of the PV cell is the single diode model. Because it is efficient and offers a good balance in accuracy, this is taken into consideration for PV system modelling in this work. Fig. 1 shows this model's corresponding circuit.

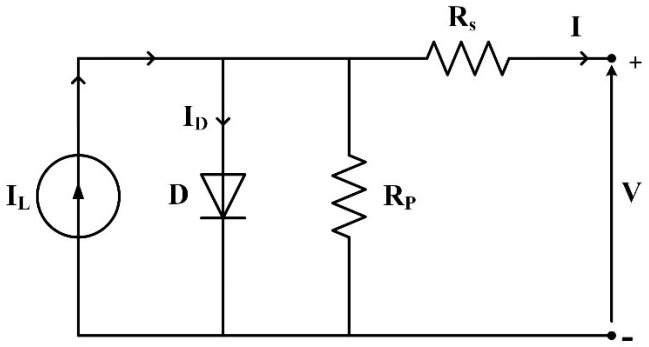

Fig.2 PV Cell's representation

The PV cell's current is displayed below:

$$I = I_L - I_D - \frac{V + R_s I}{R_p} \tag{1}$$

Where,

$$I_D = I_s\left[exp\left(\frac{V + R_s I}{V_t a}\right) - 1\right] \tag{2}$$

$$I = I_L - I_s\left[exp\left(\frac{V + R_s I}{V_t a}\right) - 1\right] - \frac{V + R_s I}{R_p} \tag{3}$$

Where, $V_t = kT / q$

The following equation states that the photocurrent of a photovoltaic cell is proportional to sun irradiance and is additionally affected by temperature,

$$I_L = (I_{Ln} + K_i \Delta T)\frac{G}{G_n} \tag{4}$$

The diode saturation current I_s is given by

$$I_s = I_{sn}\left(\frac{T_n}{T}\right)^3 exp\left[\frac{qE_g}{aK}\left(\frac{1}{T_n} - \frac{1}{T}\right)\right] \tag{5}$$

$$I_{sn} = \frac{I_{scn}}{exp\left(\frac{V_{ocn}}{aV_{tn}}\right) - 1} \tag{6}$$

The Rs (series) and Rp (parallel resistance) in equation (1), are determined iteratively by aligning the model's calculated maximum power with the datasheet's peak power at the MPP. By varying voltage (V) from 0 to Vocn/Ns and solving equation (1) numerically, corresponding current (I) values are obtained. The P–V curve for the module is then derived by multiplying the voltage (V) by N_s (series-linked cells) and the current (I) by N_p (parallel-linked cells).

2.2 Partial Shading in PV Modules

PSC occur when some PV modules in an array receive different levels of irradiance due to obstacles like clouds, buildings, trees, or dirt accumulation. Unlike uniform shading, PSC runs to multiple power peaks in the P-V curve, making it challenging to trace the MPP. This happens due to shaded solar cells generate less current than unshaded ones, causing bypass diodes to activate and alter the characteristics of the array. As a result, conventional MPPT methods often get stuck in local maxima, reducing the overall power output and system efficiency. To address this issue, advanced MPPT techniques based on intelligent optimization algorithms are employed, ensuring efficient power extraction under dynamic and complex shading patterns. The shading pattern is analysed with two cases , Case-1 PSC Pattern-1, (1000 W/m^2, 300 W/m^2,600 W/m^2), Case-1 PSC Pattern-1, (700 W/m^2, 200 W/m^2,900 W/m^2).

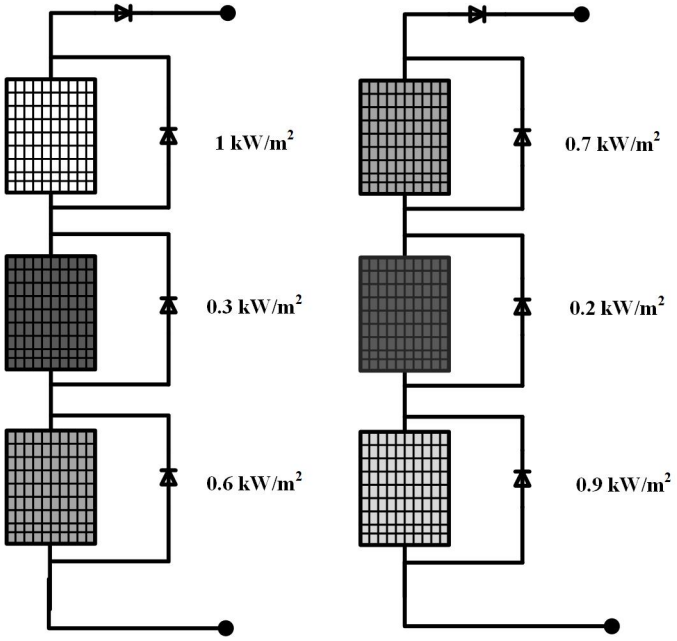

Fig.3 Different cases of shading patterns

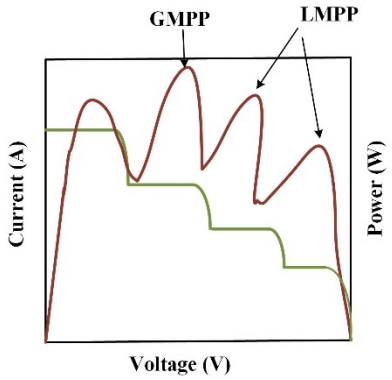

Fig.4 Characteristics of PV during Partial shading

3. MPPT Algorithms

The Following MPPT in this work are considered to analyse the PV module during partial shading conditions

3.1 PSO

PSO, a population-based evolutionary algorithm, excels in solving multi-peak engineering optimization problems, outperforming other methods in extracting global MPP under PSC. Its advantages include simplicity, ease of implementation and adjustable control variables. PSO employs a swarm of particles looking for the best outcome, drawing inspiration from bird behaviour. Based on its own and other people's experiences, each particle modifies its speed, exchanging data to maximize. Using current position, velocity, and ranges to P_{best} and G_{best}, particle migration adheres to a straightforward rule. G_{best} is the best solution for the swarm, whereas P_{best} is the finest outcome for a particle. In this case, PV output power acts as the fitness function, while particle location stands in for converter duty cycle.

$$d_i^{k+1} = d_i^k + v_i^{k+1} \tag{7}$$

$$v_i^{k+1} = wv_i^k + c_1 r_1\left(P_{best} - d_i^k\right) + c_2 r_2(G_{best} - d_i^k) \tag{8}$$

Where, v_i represents the velocity component while w signifies the inertial weight. c_1 and c_2 act as coefficients, whereas r_1 and r_2 are random values.

3.2 Adaptive PSO (APSO)

The PSO algorithm needs strong global search capabilities early on to avoid local optima and precise local search abilities later for better accuracy. Particles should start widely dispersed to explore more areas. an APSO algorithm with an adaptive strategy, featuring an asynchronous learning factor and an adaptive inertia weight factor. The initial positions of four particles are set uniformly between 0.1 and 0.7.

$$\omega = \begin{cases} \omega_m - \frac{(\omega_{max} - \omega_m)(f - f_{min})}{f_{avg} - f_{min}}, f \leq f_{avg} \\ \omega_{max}, f > f_{avg} \end{cases} \tag{9}$$

Here, f is the particle's current fitness, ω_{max} (0.6) is the inertia weight upper limit, ω_m (0.3) is a specific inertia weight, f_{avg} and f_{min} average & minimum fitness.

Asynchronous Learning Factors

In PSO, *c1* (individual learning factor) shows how particles learn from their own paths, while *c2* (social learning factor) reflects learning from the group. High *c1* in traditional PSO causes slow convergence and local wandering, while high *c2* leads to premature convergence to local optima. Fixed *c1* and *c2* values struggle to balance local and global search. In APSO, *c1* starts large for individual exploration and decreases, while *c2* starts small and increases for group-based accuracy later.

$$c_1 = c_{1min} + c_{1max}.cos\left(\frac{iter.\pi}{2.iter_{max}}\right) \tag{10}$$

$$c_2 = c_{2min} + c_{2max}.sin\left(\frac{iter.\pi}{2.iter_{max}}\right) \tag{11}$$

In (9) and (10), c_{1max} & c_{1min} is upper and lower limit of the c1, $iter.\pi$ & $iter_{max}$ is the index, and upper bound.

Convergence Condition and Restart Condition

APSO stops iterating when the distance between any two particles is below 0.003, enabling fast convergence to the MPP without hitting the iteration limit. In dynamic partial shading, changing irradiance requires reinitialization if light intensity shifts rapidly, as current particle positions and velocities become outdated. Restarting APSO finds a new maximum power point (MPP) when ΔP exceeds 1%.

$$\Delta P = \frac{|P_1 - P|}{P} \tag{12}$$

In (12), P & P_1 are the power output before restart & power after PV irradiance change.

3.3 Cuckoo Search

The optimization method CS is centered on the parasitic breeding approach used by cuckoo birds. It has been observed that a cuckoo species employ in brood parasitism, which entails laying eggs in other birds' nests (host birds).

Lévy's Flight Locating a applicable host bird's nest is crucial for cuckoo reproduction. The search for food, which occurs at random & it is typically analogous to the search for the nest. Generally speaking, animals follow trails or curves that may be described by numerical functions when they are hunting. The Lévy flight is one of the most often used models. This approach for optimization problems makes advantage of this feature. In CS, levy flying is often used to explain how cuckoos locate their nests. In mathematical terms, a Lévy flight is a arbitrary walk-in with step sizes determined by a power law derived from the Lévy distribution.

$$y = l^{-\lambda} \tag{13}$$

Where k is the variance and l is the flight time. The variance of y is infinite since l < k < 3. The stages are composed of several little steps and, occasionally, large-step, long-distance jumps according to the Lévy distribution.

In certain situations, especially for multimodal, nonlinear problems, these big hops may significantly increase the search effectiveness of cuckoo search when compared to alternative meta-heuristic processes.

(1) Cuckoos deposit their eggs in a nest that is chosen at random, one at a time.

(2) The next generation will inherit the nicest nest and the highest-quality eggs.

(3) A fixed number of nests exist, and the host bird has a probability Pa (where 0<Pa<1) of detecting cuckoo eggs. If a cuckoo egg is detected, the host bird will either throw it away or abandon the nest and build a new one. This action generates a new solution. A new result $x_i^{(t+1)}$ for a cuckoo, the Lévy flight is moved out using the following equation.

$$x_i^{(t+1)} = x_i^t + \alpha \oplus Levy(\lambda) \tag{14}$$

For a given sample number i and number of repetitions t, the step size α>0influences the adjustment of samples or eggs x_i^t. Appropriate adjustments are necessary to meet optimization restrictions and get the desired step size, frequently by using the formula given in Equation (14)

$$\alpha = \alpha_0(x_j^{(t)} - x_i^{(t)}) \tag{15}$$

The initial step change is represented by α_0 . Equation (15) calculates the next step size built on the variation among the two samples. The formula of Lévy (k) is obtained by equation (16).

$$Levy(\lambda) \approx u = l^{-\lambda}, (1 < \lambda < 3) \tag{16}$$

Relevant factors is selected for the search in order to retain CS to build MPPT. In this instance, the samples are given as the PV voltage values, n represents the samples. New voltage samples are created when the Lévy flight is finished.

$$V_i^{(t+1)} = V_i^t + \alpha \oplus Levy(\lambda) \tag{17}$$

Where $\alpha = \alpha_0(v_{best} - v_i)$, A streamlined levy distribution scheme is offered as

$$s = \alpha_0(v_{best} - v_i) \oplus Levy(\lambda) \approx k \times \left(\frac{u}{|v|^{\frac{1}{\beta}}}\right)(v_{best} - v_i) \tag{18}$$

$$u \approx N(0, \sigma_u^2) \quad v \approx N(0, \sigma_v^2) \tag{19}$$

The changing σ_u and σ_v are distinguished as

$$\sigma_u = \left(\frac{\Gamma(1+\beta) \times \sin(\pi \times \beta / 2)}{\Gamma\left(\frac{1+\beta}{2}\right) \times \beta \times 2^{\left(\frac{\beta-1}{2}\right)}}\right) and\ \sigma_v = 1 \tag{20}$$

It operates by sampling power at different voltage levels and selecting the highest power as the best sample. The remaining samples, except the best one, have a probability Pa of being discarded and replaced with new random samples. This process continues with re-evaluation of power and calculation of the objective function J until all samples converge to the MPP.

3.4 Flower pollination

This procedure is based on how pollination occurs in flowers. As is well known, pollination is a physiological process that occurs naturally during plant mating. It has to do with pollinators, such as insects, spreading pollen. The two primary forms of pollination are thought to be self and cross pollination. When pollen from one bloom fertilizes another, this is known as self-pollination. Conversely, when pollen grains are moved from one plant to another, it is known as cross-pollination. From a different perspective, flowers use a variety of strategies to disperse their pollen. Abiotic pollination is the first technique, in which the wind facilitates the spread of pollen. Biologic pollination, which occurs through insects and animals, is the second technique.

The continued existence of the fittest is the primary objective of floral pollination, according to the theory of biological evolution. Furthermore, as well as to the fittest, the optimal number of plants should be reproduced should be regarded as a significant goal. This might be seen as a plant species optimization technique. The following four guidelines need to be considered when designing and developing the FPA algorithm:

1. Pollen-carrying pollinators may travel great distances in accordance with Lévy flights, thus biotic and cross-pollination are measured to be global pollination processes.
2. Both self and biotic pollination have been regarded as local pollination.
3. A reproduction chance that is proportional to the resemblance of the 2 flowers implicated is said to be analogous to floral constancy.
4. Switch probability has been used to adjust the switching among local and global pollination.

As fellows, the mathematical models may be derived from earlier rules.

The following mathematical equation may be used to represent the global pollination

$$x_i^{t+1} = x_i^t + \gamma L(\lambda)(g_* - x_i^t) \tag{21}$$

$$L \approx \frac{\lambda \Gamma(\lambda) \sin\left(\frac{\pi\lambda}{2}\right)}{\pi} \frac{1}{s^{1+\lambda}} (s \gg s_0 > 0) \tag{22}$$

The following is a mathematical representation of the second and third principles for local pollination.

$$x_i^{t+1} = x_i^t + \in (x_j^t - x_k^t) \tag{23}$$

Where x_j^t, x_k^t are pollen from different flowers. If x_j^t and x_k^t are picked from a uniform distribution in [0,1], then this likewise turns into a local random walk if they are members of the same species or population. Activities related to FPA can occur at many sizes, including local and global. The ideal duty cycle that corresponds to the PV system's global MPP is extracted.

3.5 Grey Wolf

This procedure mimics the hunting manners and leadership chain of command of grey wolves to resolve optimization issues. The hierarchy comprises of 4 types of wolves: (α) representing the best solution, (β) as the 2nd-best, (δ) as the third, and (ω) representing the rest of the population. The optimization process involves 3 major steps: searching, encircling, and attacking the prey, where α leads the hunt, followed by β and δ, while ω supports the pack. This strategy is effectively applied in MPPT for PV modules to optimize power extraction under dynamic conditions. To mitigate fluctuations, the GWO is employed to maintain a constant duty cycle at MPP.

The following equation is used to simulate the entire grey wolf hunting method as explained above.

$$\vec{E} = \left| \vec{C}.\vec{X_p}(t) - \vec{X_p}(t) \right| \tag{24}$$

$$\vec{X}(t+1) = \vec{X_p}(t) - \vec{F}.\vec{E} \tag{25}$$

In this case, t stands for the current repetition, and the coefficient vectors are given by E, F, and C. The hunting prey's position vector is represented by Xp, while the GW vector is shown by X. The following is how the vectors F and C are calculated:

$$\vec{F} = 2\vec{a}.\vec{r_1} - \vec{a} \tag{26}$$

$$\vec{C} = 2.\vec{r_2} \tag{27}$$

To mitigate fluctuations and losses present in traditional MPPT procedures, the d is normalized at MPP to a constant value. The d is regarded as the gray wolf in the GWO MPPT implementation.

$$d_i(k+1) = d_i(k) - F.E \tag{28}$$

$$P(d_i^k) > P(d_i^{k-1}) \tag{29}$$

In this case, P is the power, i for the number of individual GW that are currently in existence, and k for the number of iteration.

3.6 Horse Herd optimization

To make the HHO function, the behaviour of horses in their natural environments is investigated. In their behaviour (F), horses commonly exhibit grazing (A), defensive mechanisms (D), socialization (C), hierarchical (B), and imitation (E). The transfer given to horses at each repetition is stated in equation (30).

$$Z_i^{iter,AGE} = S_i^{iter,AGE} + Z_i^{(iter-1),AGE}, AGE = \alpha,\beta,\gamma,\delta \tag{30}$$

The precise position of the i_{th} stallion is shown by $Z_x^{iter,AGE}$,the stallion's age range is displayed by AGE, and the current replication is represented by Iter. $S_i^{iter,AGE}$ illustrates the velocity vector of horse. Horses specified by α, β, γ, and δ, respectively based on their age.

This constant feeding pattern is referred to as "continuous eating." In pastures, you could see mares grazing with their young. Using a grass coefficient, the HOA approach determines how much grazing space each horse needs. A particular formula may be used to describe the grazing behaviour of horses of various ages that are observed grazing in pastures.

$$A_i^{iter,AGE} = a_i^{iter,AGE} \times \left(U + R \times L\right) \times \left(Z_i^{(iter-1)}\right), AGE = \alpha,\beta,\gamma,\delta \quad (31)$$

$$a_i^{iter,AGE} = a_i^{(iter-1),AGE} \times w_a \quad (32)$$

The HHO is inspired by the grazing and hierarchical behaviour of wild horses, where their movement is influenced by a motion parameter w_a and a random factor R ranging from 0 to 1, causing non-linear movement per iteration. In nature, horses follow a leader, typically an experienced mare or stallion, demonstrating a clear hierarchical structure. This leadership tendency is represented by a coefficient *h* in HOA, reflecting the herd's inclination to follow the brightest and most qualified horse. Studies on horses aged five to fifteen validate this hierarchical behaviour, which is effectively utilized in optimization processes

$$B_i^{iter,AGE} = b_{iter}{}^{iter,AGE} \times \left(Z_*^{(iter-1)} - Z_i^{(iter-1)}\right), AGE = \alpha,\beta,\gamma \quad (33)$$

$$b_i^{iter,AGE} = b_i^{(iter-1),AGE} \times w_b \quad (34)$$

$B_i^{iter,AGE}$ shows how the superior horse position has a large effect on the velocity parameter, while $Z_*^{(iter-1)}$ disp shows where the best horse is actually located.

Horses live among other creatures, often sharing homes, which exposes stallions to predators but offers herd security. Pluralism aids survival and independence. Their social nature sparks frequent fights, while excitability reflects individuality. Some horses prefer companionship with cattle and sheep over isolation, gravitating toward the herd's center. Young horses are notably sociable, aligning with the phrase "particularly gregarious."

$$C_i^{iter,AGE} = c_{iter}{}^{iter,AGE} \times \left(\left(\frac{1}{N}\sum_{k=1}^{N} Z_k^{(iter-1)}\right) - Z_i^{(iter-1)}\right), AGE = \beta,\gamma \quad (35)$$

$$c_i^{iter,AGE} = c_i^{(iter-1),AGE} \times w_c \quad (36)$$

The i_{th} social velocity vector is $C_i^{iter,AGE}$, whereas the coordination of the i_{th} iteration with the herd is reflected in $c_i^{iter,AGE}$. It falls by a w_c factor with each iteration. The lifelong tendency of a young horse to imitate its elders is represented by the following equation:

$$E_i^{iter,AGE} = e_{iter}{}^{iter,AGE} \times \left(\left(\frac{1}{pN}\sum_{k=1}^{pN} Z_k^{(iter-1)}\right) - Z_i^{(iter-1)}\right), AGE = \gamma \quad (37)$$

$$e_i^{iter,AGE} = e_i^{(iter-1),AGE} \times w_e \quad (38)$$

Horses react to predators with a fight-or-flight response, preferring to flee but bucking if trapped. They protect their territory from threats like foxes. Their defence prevents encounters with other horses in the HOA operation, and factor d is essential. They either run away or remain steadfast when threatened. By avoiding mispositioning, the algorithm's negative coefficient guarantees safety.

$$D_i^{iter,AGE} = -d_{iter}{}^{iter,AGE} \times \left(\left(\frac{1}{qN}\sum_{k=1}^{qN} Z_k^{(iter-1)}\right) - Z_i^{(iter-1)}\right), AGE = \alpha,\beta,\gamma \quad (37)$$

$$d_i^{iter,AGE} = d_i^{(iter-1),AGE} \times w_d \quad (39)$$

Where the i_{th} stallion's outflow vector, $D_i^{iter,AGE}$ is calculated by averaging the placements of the $Z_k^{(iter-1)}$ vector. The entire amount of horses in the most severe case is also included in QN. According to different estimates, 20% of all horses are q. The factor of a decrease is denoted by w_d.

Horses graze for hours, shifting between pastures. Though often stabled, they wander to explore, driven by curiosity and aided by sidewall observation. In modelling, this is represented as arbitrary behaviour times factor *r*. Wandering starts young and grows with maturity.

$$F_i^{iter,AGE} = f_{iter}{}^{iter,AGE} \times \mathcal{P}\left(Z_i^{(iter-1)}\right), AGE = \gamma,\delta \tag{40}$$

$$f_i^{iter,AGE} = f_i^{(iter-1),AGE} \times w_f \tag{41}$$

For local search, $F_i^{iter,AGE}$ represents the i_{th} horse's arbitrary velocity vector, whereas w_f denotes a decreasing factor of $f_i^{iter,AGE}$ each cycle.

The age-specific horse velocity vector using the following formula.

$$S_i^{iter,\alpha} = A_i^{iter,\alpha} + D_i^{iter,\alpha} \tag{42}$$

$$S_i^{iter,\beta} = A_i^{iter,\beta} + B_i^{iter,\beta} + C_i^{iter,\beta} + D_i^{iter,\beta} \tag{43}$$

$$S_i^{iter,\gamma} = A_i^{iter,\gamma} + B_i^{iter,\gamma} + C_i^{iter,\gamma} + E_i^{iter,\gamma} + D_i^{iter,\gamma} + F_i^{iter,\gamma} \tag{44}$$

$$S_i^{iter,\delta} = A_i^{iter,\delta} + E_i^{iter,\delta} + F_i^{iter,\delta} \tag{45}$$

3.7 Hybrid PO-PSO

The Hybrid PO-PSO MPPT process reduces steady-state oscillations and improves tracking efficiency by combining the benefits of both approaches. The algorithm functions in two primary stages:

Initial Global Search Using PSO: The MPP is initially explored throughout a broad range using the PSO algorithm. A swarm of particles is started with arbitrary placements and velocities, each of which represents a potential duty cycle of the converter. Using velocity and position update equations, the particles update their positions according to the G_{best} and their individual best-known P_{best}. The system is swiftly guided to an ideal area of the power curve by this global search.

Fine-Tuning Using PO: The PO procedure takes over for local refining when PSO finds a near-optimal operating point. PO monitors the variation in power output that effects from perturbing the duty cycle. The perturbation proceeds in the same direction if the power increases; if not, it reversals. This adjustment enhances steady-state performance and reduces power oscillations.

4. Simulation Results & Discussions

The simulation of the comparative assessment is carried out in 2 cases in MATLAB considering the different irradiance pattern

4.1 Case-1 Partial shading Pattern-1 (PSC-1 1000 W/m2, 300 W/m2,600 W/m2)

Fig.4 represents the power output of a PV modules under PSC-1 using different MPPT procedures. The primary goal of these algorithms is to trace the GMPP and obtain the possible power from the PV array despite shading effects. In this case the GMPP is 104.5W. It can be observed that each algorithm has a different response time and power tracking efficiency. Some algorithms exhibit higher fluctuations and slower convergence, while others demonstrate faster convergence to the MPP with minimal oscillations. Among these procedures, the Hybrid PO-PSO shows superior performance by quickly converging to the maximum power point with minimal power loss. This indicates that the Hybrid PO-PSO approach is more effective in handling the complex power curves caused by partial shading conditions, ensuing in a higher and more stable power from the PV module. The Load power obtained at PSC-1 is shown in Fig.5.

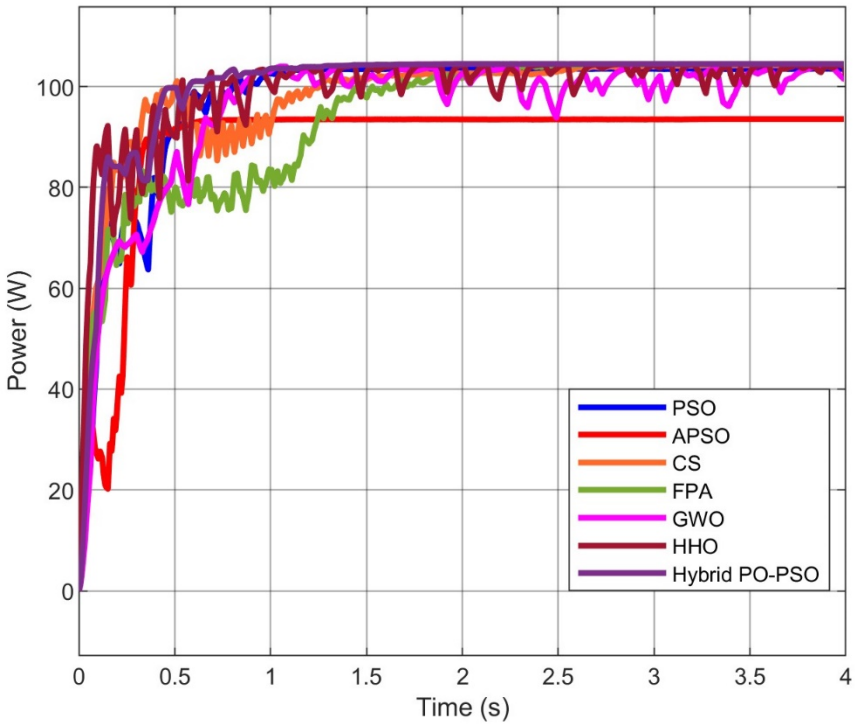

Fig.4 Comparison of PV Powers at PSC-1

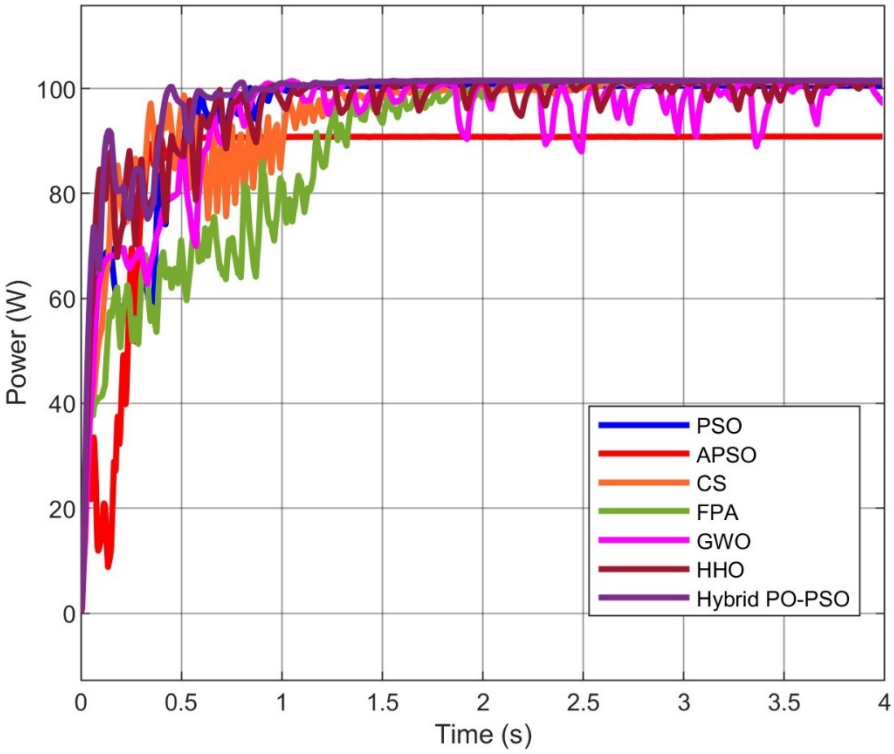

Fig.5 Comparison of Load Powers at PSC-1

Table.1Tracking Efficiency, PV& Load Power at PSC-1

MPPT	PV Power Obtained (W)	Tracking Efficiency(%)	Load Power (W)
PSO	103.5	99.04	100.6
APSO	93.4	89.46	90.8
CS	104	99.52	101.1
FPA	104.4	99.90	101.5
GWO	100.3	95.98	98.46
HHO	104.3	99.81	101.3
Hybrid PO-PSO	104.5	100	101.5

Table 1 presents the performance comparison of various MPPT under PSC-1. The Hybrid PO-PSO method achieves the highest tracking efficiency (100%) and PV power output (104.5 W), followed closely by FPA and HHO with tracking efficiencies of 99.90% and 99.81%, respectively. The CS and PSO methods also perform well, with efficiencies above 99%. In contrast, APSO records the lowest efficiency 89.46%, resulting in lower PV and load power outputs. This indicates that Hybrid PO-PSO is the most effective approach under PSC-1, ensuring maximum power extraction and delivery to the load.

4.2 Case-2 Partial shading Pattern-2 (700 W/m2, 200 W/m2,900 W/m2)

The results of PV scheme under PSC-2 using various MPPT a procedures. In this case the GMPP is 119.5W It is observed that different algorithms exhibit varying performances considering the tracking efficiency. Some algorithms effectively track the GMPP, resulting in higher and more stable power outputs, while others show slower convergence or remain stuck at an LMPP. In this case, the FPA algorithm fails to track the GMPP and remains trapped in a local maximum, leading to significantly lower power extraction compared to other algorithms. This behaviour highlights the limitation of the FPA algorithm under complex PSC , where multiple peaks in the power curve exist. The Hybrid PO-PSO exhibits superior performance by rapidly converging to the GMPP with minimal oscillations, ensuring maximum power extraction under shading conditions. Other algorithms such as PSO, APSO, and HHO also demonstrate good performance but show relatively higher power fluctuations during the tracking process. The Load power obtained at PSC-1 is displayed in Fig.7.

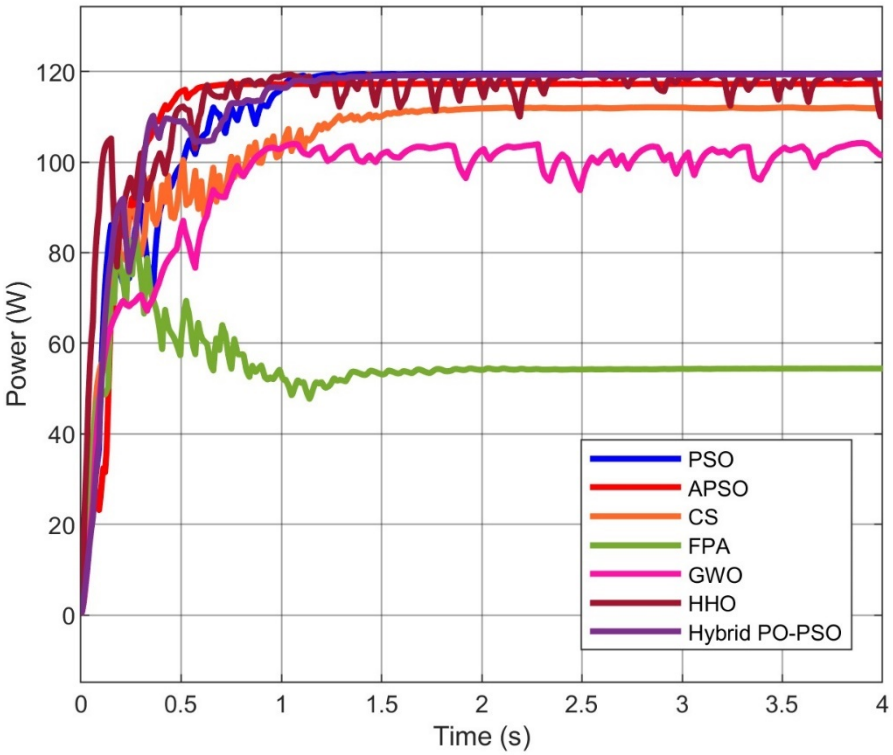

Fig.6 Comparison of PV Powers at PSC-2

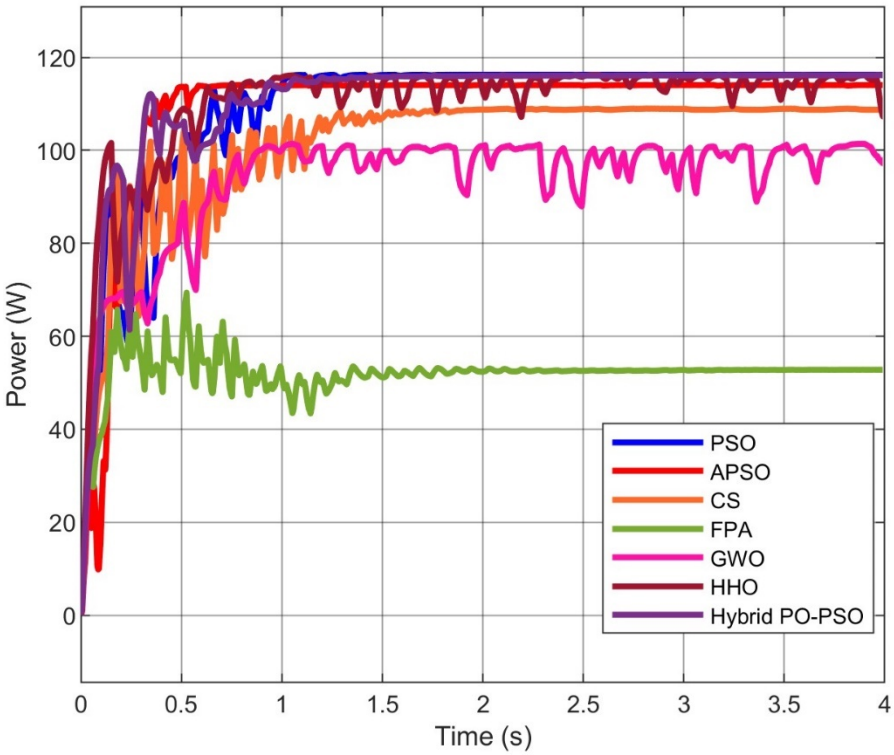

Fig.7 Comparison of Load Powers at PSC-2

Table.2 Tracking Efficiency, PV& Load Power at PSC-2

MPPT	PV Power Obtained (W)	Tracking Efficiency(%)	Load Power (W)
PSO	119.4	99.92	116.3
APSO	117.3	98.16	114.1
CS	112.1	93.81	108.9
FPA	54.3	45.44	52.76
GWO	100.3	83.93	98.4
HHO	119	99.58	115.7
Hybrid PO-PSO	119.3	99.83	116.1

Table 2 compares the MPPT techniques under PSC-2. Hybrid PO-PSO, PSO, and HHO demonstrate the highest tracking efficiencies, exceeding 99%, ensuring optimal PV power extraction near 119 W. APSO also performs well with 98.16% efficiency. However, methods like FPA and GWO show significantly lower tracking efficiencies (45.44% and 83.93%, respectively), leading to reduced power output. The results highlight that Hybrid PO-PSO maintains superior performance across different shading conditions, achieving near-optimal power extraction and delivery compared to other MPPT procedures

5. Conclusion

The Hybrid PO-PSO MPPT exhibits superior working in tracing the MPP under PSC. By integrating the PO method with PSO, this hybrid approach effectively links the fast local tracking capability of PO with the global search ability of PSO. This ensures accurate and efficient MPP tracking while minimizing power losses and steady-state oscillations. Under PSC-1 (irradiance: 1000 W/m², 300 W/m², 600 W/m²), Hybrid PO-PSO achieves the highest tracking efficiency of 100%, extracting 104.5 W of PV power and delivering 101.5 W to the load. In PSC-2 (irradiance: 700 W/m², 200 W/m², 900 W/m²), the algorithm maintains a high tracking efficiency of 99.83%, successfully extracting 119.3 W of PV power and delivering 116.1 W to the load. These results confirm that Hybrid PO-PSO consistently finds the GMPP faster than other algorithms while avoiding local maxima. The key advantage of Hybrid PO-PSO lies in its ability to rapidly respond to dynamic shading conditions and track the optimal power point with high accuracy. Unlike conventional MPPT methods, which may suffer from slow convergence or local optima trapping, The comparative analysis of MPPT procedures under PSC provides valuable insights into the strengths and limitations of different procedures.

References

[1] Balasubramanian, I. R., Ilango Ganesan, S., & Chilakapati, N. (2014). Impact of partial shading on the output power of PV systems under partial shading conditions. *IET power Electronics*, *7*(3), 657-666.

[2] Kumari, P. A., & Geethanjali, P. (2018). Parameter estimation for photovoltaic system under normal and partial shading conditions: A survey. *Renewable and Sustainable Energy Reviews*, *84*, 1-11.

[3] Ishaque, K., Salam, Z., & Taheri, H. (2011). Modeling and simulation of photovoltaic (PV) system during partial shading based on a two-diode model. *Simulation Modelling Practice and Theory*, *19*(7), 1613-1626.

[4] Mohapatra, A., Nayak, B., Das, P., & Mohanty, K. B. (2017). A review on MPPT techniques of PV system under partial shading condition. *Renewable and Sustainable Energy Reviews*, *80*, 854-867.

[5] Yang, B., Zhu, T., Wang, J., Shu, H., Yu, T., Zhang, X., ... & Sun, L. (2020). Comprehensive overview of maximum power point tracking algorithms of PV systems under partial shading condition. *Journal of Cleaner Production*, *268*, 121983.
[6] Rezk, H., Fathy, A., & Abdelaziz, A. Y. (2017). A comparison of different global MPPT techniques based on meta-heuristic algorithms for photovoltaic system subjected to partial shading conditions. *Renewable and Sustainable Energy Reviews*, *74*, 377-386.
[7] Sundareswaran, K., & Palani, S. (2015). Application of a combined particle swarm optimization and perturb and observe method for MPPT in PV systems under partial shading conditions. *Renewable Energy*, *75*, 308-317.
[8] Kermadi, M., Salam, Z., Eltamaly, A. M., Ahmed, J., Mekhilef, S., Larbes, C., & Berkouk, E. M. (2020). Recent developments of MPPT techniques for PV systems under partial shading conditions: a critical review and performance evaluation. *IET Renewable Power Generation*, *14*(17), 3401-3417.
[9] Eltamaly, A. M., Al-Saud, M. S., Abokhalil, A. G., & Farh, H. M. (2020). Photovoltaic maximum power point tracking under dynamic partial shading changes by novel adaptive particle swarm optimization strategy. *Transactions of the Institute of Measurement and Control*, *42*(1), 104-115.
[10] Diab, A. A. Z., & Rezk, H. (2017). Global MPPT based on flower pollination and differential evolution algorithms to mitigate partial shading in building integrated PV system. *Solar Energy*, *157*, 171-186.
[11] Shang, L., Zhu, W., Li, P., & Guo, H. (2018). Maximum power point tracking of PV system under partial shading conditions through flower pollination algorithm. *Protection and Control of Modern Power Systems*, *3*(4), 1-7.
[12] Sarwar, S., Hafeez, M. A., Javed, M. Y., Asghar, A. B., & Ejsmont, K. (2022). A horse herd optimization algorithm (HOA)-based MPPT technique under partial and complex partial shading conditions. *Energies*, *15*(5), 1880.
[13] Chowdhury, S. B. R., Gayen, P. K., Roy, S., & Babu, N. V. (2022). A Novel MPPT algorithm for PV systems under variable Shading Conditions using Horse Herd Optimization. *Journal of Electrical Systems*, *18*(1).
[14] Figueiredo, S., & e Silva, R. N. A. L. (2021). Hybrid MPPT technique PSO-PO applied to photovoltaic systems under uniform and partial shading conditions. *IEEE Latin America Transactions*, *19*(10), 1610-1617.
[15] Basiński, K., Ufnalski, B., & Grzesiak, L. M. (2017). Hybrid MPPT algorithm for PV systems under partially shaded conditions using a stochastic evolutionary search and a deterministic hill climbing. Power Electronics and Drives, 2(37/2), 49-59.